Journal of Applied Sciences and Nanotechnology, Vol. 1, No. 4 (2021)

Journal of Applied Sciences and Nanotechnology

Journal homepage: https://jasn.uotechnology.edu.iq/

Preparation of V_2O_5 and SnO_2 Nanoparticles and Their Application as Pollutant Removal

Zahra Ali Hassan, Rashed T. Rasheed*

Department of Applied Sciences, University of Technology – Iraq

Article information

Article history:
Received: June, 17, 2021
Accepted: October, 26, 2021
Available online: December, 04, 2021

Keywords:
Vanadium pentoxide nanoparticle,
Tin dioxide nanoparticles,
Pollution removal

Corresponding Author:
Rashed Taleb Rasheed
100010@uotechnology.edu.iq

Abstract

Vanadium pentoxide and Tin dioxide nanoparticles were prepared by hydrothermal methods to remove methylene blue (MB) and bromothymol blue (BTB) dyes). First the prepared nanoparticles were heated at different temperature (90 ^{o}C and 500 ^{o}C). Then these nanoparticles were characterized by different methods such as UV/Visible, FT-IR Spectroscopy, X-Ray Diffraction (XRD), Atomic Force Microscopy (AFM), and Scanning Electron Microscopy (SEM)**.** Our results explain that vanadium pentoxide nanoparticles appeared high remove activity against both types of organic dyes (MB and BTB) compared to tin dioxide nanoparticles. Furthermore,vanadium pentoxide heating at 90 ^{o}C has grain size (86.02 nm) more than that of Tin dioxide (48.02 nm) at same temperature. The activity of vanadium pentoxide is more than that of tin dioxide.may be related to high ionic potential (0.073), compared with Tin dioxide (0.048).

DOI: 10.53293/jasn.2021.3869.1049, Department of Applied Science, University of Technology

1. Introduction

Water is the essential element of life and it is a precious resource for human civilization. Clean water is a major global challenge in the twenty-first century. Thus, global climate change highlights the already unequal distribution of freshwater [1]. Clean water is water that is free from toxic substances, chemicals, and pathogens. Dyes are considered one of the most critical organic pollutants that cause water pollution and cause many diseases. The adsorption technique, is chemical adsorption, biological adsorption and ion exchange [2-4]. Nanomaterials are considered to be the absorbing materials for water pollutants by adsorption [2]. Nanotechnology has proven its presence in many fields such as sensing pollutants and water pollution, Nanomaterials such as metallic, metal oxides, carbon compounds, nanocomposites and filtering membranes have been used for filtering membranes in wastewater treating [5].metal oxides such as(Al_2O_3, V_2O_5, Mn_2O_3, SnO_2, La_2O_3 are used in water purification technology due to their ability to separate the chemical and biological properties of water [6]. The dye absorption is done on the surface of nano absorbent materials. Carbon nanotubes, graphene, zeolites and nanocomposites have higher efficiency and larger surface areas. First the contaminants are absorbed on the surface of the nanoparticles, then the solution is accompanied by a change in the pH, a change in temperature, *etc*.[7].

2. 2. Experimental Procedure

2.1 Preparation of Vanadium Pentoxide Nanoparticles (V_2O_5 NPs)

Vanadium pentoxide was prepared by the hydrothermal (reflex) method by dissolving 2 grams of ammonium metavanadate (NH_4VO_3) in a mixed solution of distilled water and ethanol in a ratio of a ratio (7:3) with add 0.5 of cetyltrimethylammonium bromide (CTAB) and drops of nitric acid(HNO_3) until it reaches the pH of 2.5, heat the solution for 6 hours, then washed several washes after the reaction ends, dried at 90 °C and annealed at 500°C for 2 hours [8, 9].

$$2NH_4VO_3 + 2HNO_3 + nH_2O \xrightarrow[CTAB]{CH_3CH_2OH} V_2O_5nH_2O + 2NH_4NO_3 + H2O \quad (1)$$

$$V_2O_5nH_2O \xrightarrow{90\,^{\circ}C} V_2O_5.1.8H_2O + (n-1.8)H_2O \quad (2)$$

$$V_2O_5.1.8H_2O \xrightarrow{500^{\circ}C} V_2O_5 + 1.8H_2O \quad (3)$$

2.2 Preparation of Tin Dioxide Nanoparticles (SnO_2 NPs)

Tin dioxide was prepared using the hydrothermal method (autoclave) by dissolving two grams of Tin tetrachloride ($SnCl_4$) in distilled water, adding to it 0.92 g of urea and 0.5 g of cetyltrimethylammonium bromide (CTAB) placing it with an autoclave for 12 hours at 200 and washed several washes and dried at 90 and annealed at 500 for two hours [10].

$$NH_2CONH_2 + 3H_2O \longrightarrow 2NH_2OH + CO_2 \quad (4)$$

$$SnCl_4 + 2NH_4OH \xrightarrow{autoclave} Sn(OH)_4 + 4NH_4Cl \quad (5)$$

$$Sn(OH)_4 \xrightarrow{autoclave} SnO_2 + 2H_2O \quad (6)$$

2.3 The adsorption of methylene blue (MB) / or bromothymol blue (BTB) dyes.

We performed two experiments to verify the adsorption of two organic dyes (methylene blue (MB) and bromothymol blue (BTB)). 0.1 g of each nanoparticle (V_2O_5 and SnO_2) was added to 25 ml (20 mg/l) of the dye solutions (MB or BTB) in concentration ($4x10^{-5}$ M, $64x10^{-5}$ M) respectively. The first experiment was to adsorption of methylene blue (MB) dye onto nanoparticles. The second experiment was to adsorption of bromothymol blue (BTB) dye onto nanoparticles. In these two experiments, we used our nanoparticles after heating at 90 ^{o}C and 500 ^{o}C. The removal percentages (R%) of MB / or BTB dyes onto nanoparticles were calculated through the equation (7) [8].

$$(R\%) = [(C_o - C_t)/C_o] \times 100\ \% \quad (7)$$

Where; C_o indicates the initial concentration of the dye mg/L, and C_t indicates the final concentration of the dye mg/ L.

The adsorption capacity (q_t) of the MB/ or BTB dyes onto nanoparticles was calculated through equation (8).

$$q_t = (C_o - C_t)\ V/\ W \quad (8)$$

Where; W indicates weight in grams of nanoparticles, V volume of dye solution in millilitres.

3. Results and Discussion

3.1 Optical properties of the nanoparticles solutions.

The optical properties of the prepared nanoparticle solutions (10^{-5} M**)** were done by dissolved the nanoparticle in Dimethylsulfoxide (DMSO) solvent. The plot of optical transmission curves against the wavelength for nanoparticles at different temperatures (90 °C and 500 °C,) from the region between 200 nm to 800 nm is explained in figure (1). The spectrum of vanadium pentoxide (figure (1-a)) shows the transmittance edge is shifted to a lower wavelength (blue shift) from 480 nm to 320 nm with an increase of annealing temperatures. We can produce the value of the energy gap (the space between HOMO and LUMO) according to the following experiment equation:

$$\text{Energy gap (eV)} = 1240/\lambda_{max} \qquad (9)$$

Where 1240 is a factor that converts nm to eV, λ_{max} is the first maximum transmittance in nm. Therefore, the energy gap of $V_2O_5.nH_2O$ equal to 2.583 eV and that annealing at 500 ^oC (V_2O_5) equal to 3.875 eV respectively. These results are agreed with reference [11] which found equal to 2.63 eV and 3.48 eV at temperature 90 ^oC and 500 ^oC respectively..

The tin dioxide nanoparticles show a decrease in the transmittance edge (blue shift), from 347 nm to 339 nm, annealing temperatures, this may be relating to converting the as-prepared (tin hydroxide) nanoparticles to tin dioxide throw autoclave reaction. Therefore, the energy gap of as-prepared equal to 3.573 eV and that of annealing at 500 ^oC equal to 3.657 eV respectively, as in figure (1 –b). These results are agreed with reference [12] which is due to the fundamental absorption of light.

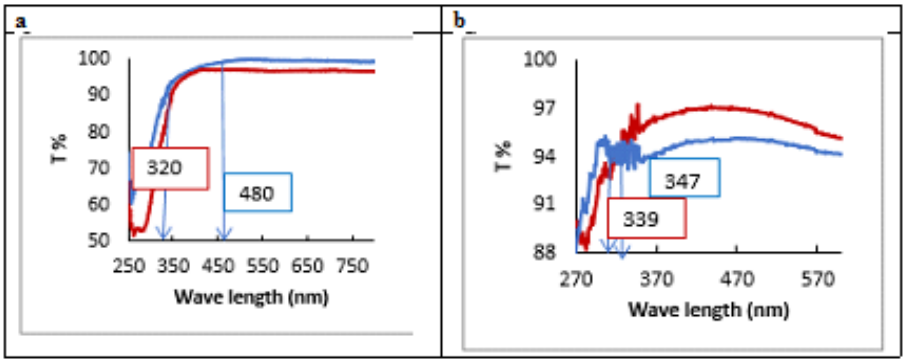

Figure (1): The optical transmittance for nanoparticles, a: vanadium pentoxide; b: tin dioxide; annealing at different temperatures (90 °C and 500 °C).

3.2 Fourier Transform Infrared Spectroscopy (FTIR)

3.2.1 FTIR Spectra for $V_2O_5.nH_2O$ and V_2O_5 nanoparticles

The FTIR spectrum of vanadium pentoxide nanoparticles (as-prepared) $V_2O_5.nH_2O$ that heated at 90 **°C** for 60 min explains in figure (2-a). The broadband at 3203 cm^{-1} relates to stretching vibration and the peak at 1610 cm^{-1} relate to bending of the O-H group in the water. The peaks at 1404 cm^{-1}, 1004 cm^{-1}, 964 cm^{-1} and 837 cm^{-1} corresponding to the bending vibration of C=C vibration of CTAB, vanadyl stretching of (δ V-O), V=O vibration [13], and V-O-V vibration respectively. The bands at 717 cm^{-1} and 626 cm^{-1} corresponding to the asymmetric and symmetric stretch around V-O-V. Figure (2-b) shows V_2O_5 annealing at 500**°C** for 120 min, there are no peaks that appeared to relate to water in this sample. The peaks at 1016 cm^{-1} correspond to stretching vibration of V=O and that at 812 cm^{-1} relate to stretching of V-O-V and that at 648 cm^{-1} correspond to V-O stretching [14].

3.2.2 FTIR Spectra for SnO_2 nanoparticles

Figures (2-c and 2-d) show the FTIR spectra of SnO_2 as prepared and annealed at 500 ^oC. There are no high differences between both spectra, which means both compounds are the same (SnO_2). These may relate to converting tin hydroxide ($Sn(OH)_4$) to tin dioxide (SnO_2) during the reaction proses in the autoclave, due to the high reaction temperature (200 ^oC). The broad peaks around 3400 cm^{-1} and 1631 cm^{-1} correspond to O-H bond's stretching and bending in water in water respectively. The broad peak at 544 cm^{-1} assigned to the Sn–O vibration and this broad peak improves to 544 cm^{-1} [15].

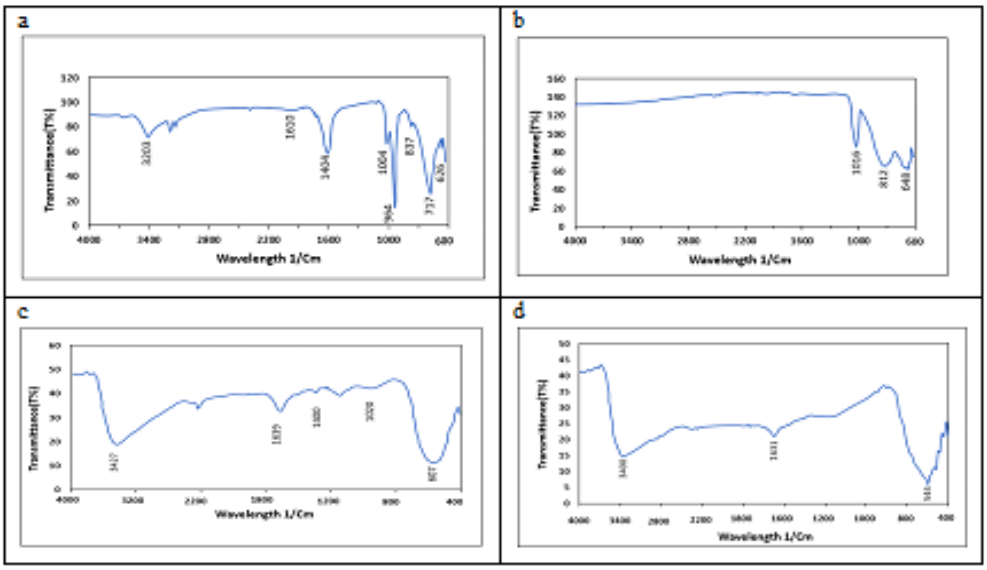

Figure (2): FTIR spectra of V_2O_5 a: as- prepared, b: annealing at 500° C and SnO_2 c: as-prepared, d: annealing at 500 ° C.

3.3 X-Ray Diffraction (XRD)

3.3.1 The X-Ray Diffraction for $V_2O_5.nH_2O$ and V_2O_5 nanoparticles

The results of the X-ray analysis of vanadium pentoxide prepared by the hydrothermal method (reflex), and heated at 90 °C, showed the main diffraction peaks at 2θ = (40.8◦, 44.81◦, 47.80◦, and 49.60◦) corresponding to the characteristic diffraction peaks of (002), (411), (600), and (302) relate to $V_2O_5.nH_2O$, and that at 2θ = 27.7 corresponding to VOOH according to the card number (JCPDS card No. 01-089-0612), as shown in figure (3-a) [16].

When annealing at 500 °C we notice the prominent diffraction peaks at 2θ = (20.15◦, 21.20◦, 25.20◦, 31.66◦, 32.03◦, 32.49◦, 34.07◦, 47.80◦, 49.60◦, 50.99◦, 54.61◦,57.92◦, 60.93◦ and 62.80◦), which corresponds to the peak's diffraction (001), (101), (110), (301), (011), (111), (310), (600), (302), (020), (121), (611), (312), and (710). Meanwhile, there are improve and increase in its density of many peaks such as those at 2θ = (20.15, 32.03, 34.07, 50.99, 60.93) which corresponds to the peak's diffraction (001), (011), (310), (020), and (312), These peaks are identical to the card number (JCPDS card no. 41-1426), as in figure (3-b) [17, 18]. The grain size of the nanoparticles has been estimated from the full width at half maximum (FWHM) of the diffraction peak using the Debye-Sherrer formula according to the equation:

$$D = K\lambda / \beta \cos\theta \qquad (10)$$

Where, (D) is crystallite size, (k) is the shape factor (≈ 0.9), (λ) is the x-ray wavelength (1.540 Å), (β) is the full width half maximum (FWHM) in radians, and (θ) is the Bragg's diffraction angle value [19]. Table (1) shows the average grain size for V_2O_5 annealed at 500 ◦C according to the Scherrer equation.

3.3.2 The X-Ray Diffraction for SnO_2 nanoparticles

The X-ray results of heated SnO_2 at 90 ^oC, is very similar to that of annealing at 500 ^oC with a slight change in intensity, this indicates that the formation of SnO_2 in both situations. The most prominent of the main peaks that appeared are 2θ = (26.45, 33.71, 51.63, 54.61, and 65.85), which corresponds to the diffraction values of (110), (101), (211), (220), and (301) as shown in the figures (3-c and 3-d). These peaks correspond to the card number (JCPDS part no. 041-1445) [20]. This indicates the sample prepared by autoclave completely converts to SnO_2 without the formation of $Sn(OH)_4$ as it happens when prepared by sol-gel. This may be related to the higher temperature (200 ^oC) used in the autoclave in preparation. Table (1) shows the average grain size for SnO_2 annealed at 500 ◦C according to the Scherrer equation.

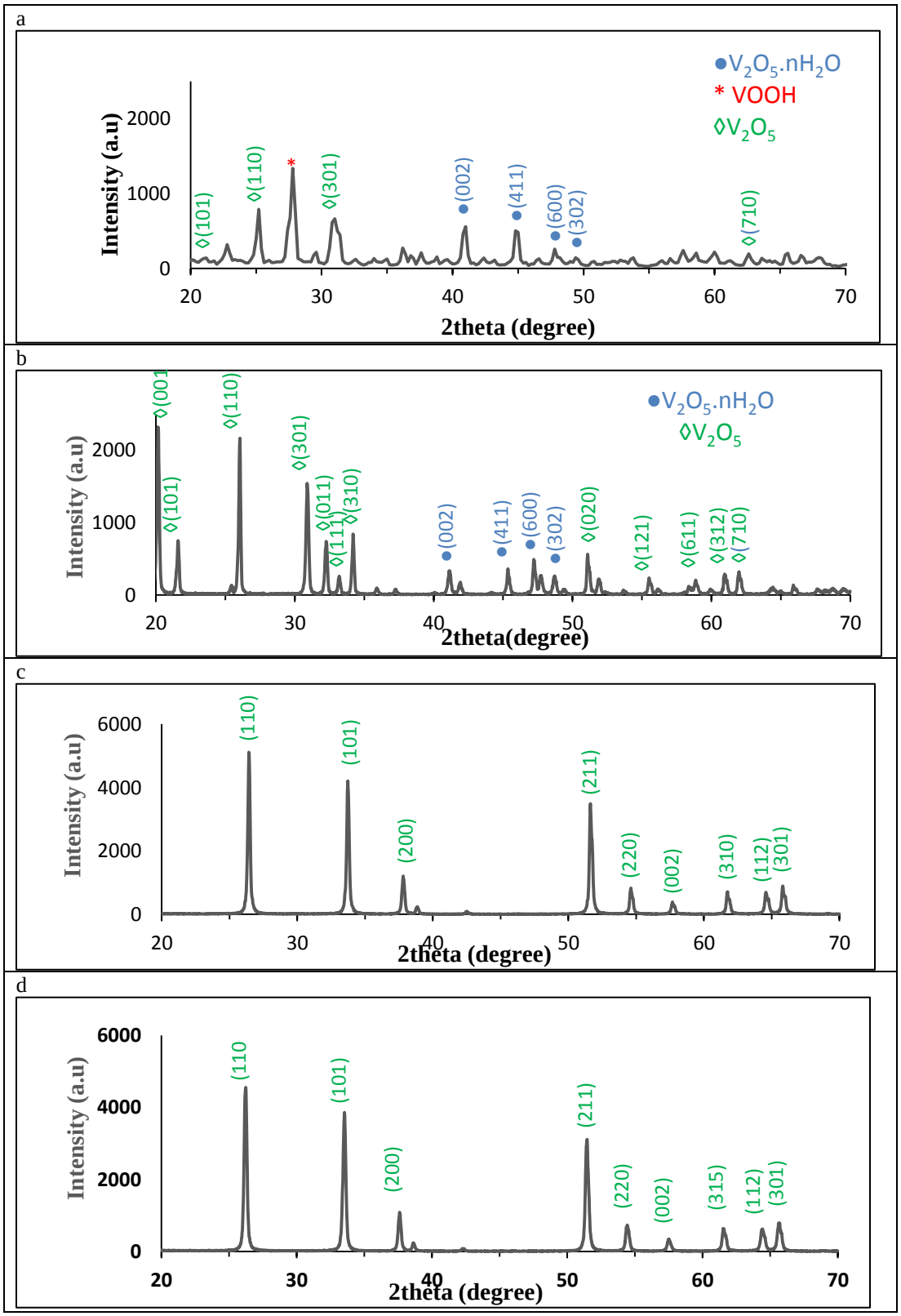

Figure (3): XRD of V_2O_5 a: as-prepared, b: annealing at 500 ^oC and SnO_2 c: as-prepared, d: annealing at 500 ^oC.

Table (1): The grain size of the V_2O_5 and SnO_2 nanoparticles calculate by the Scherer equation.

	2θ (deg)	hkl	FWHM (deg)	D(nm)
V_2O_5 annealing at 500 ◦C for 120 min	20.15	001	0.1732	45.136
	34.07	101	0.1968	38.575
	51.05	310	0.1440	49.757
SnO_2 annealing at 500 ◦C for 120 min	26.45	110	0.2125	36.373
	33.71	101	0.2362	32.171
	51.63	211	0.1968	36.319

3.4 Surface Morphology

3.4.1 By atomic force microscopy (AFM)

AFM results of vanadium pentoxide and tin dioxide in three (3D) dimension images with different temperatures as in figure (4). The distribution and accumulation of nanoparticles seem to large balls (figure 4-a) and convert to smaller when annealing at 500 ^oC (figure 4-b). This may relate to the loss of water molecules from the sample, as explained in equation [9].

$$\mathbf{V_2O_5.nH_2O \rightarrow V_2O_5 + n\,H_2O} \qquad \mathbf{(11)}$$

These results agree with the average grain size obtained from AFM analysis, which converts the average grain size from 86.02 nm ($V_2O_5.nH_2O$) to 70.34nm of V_2O_5 when the heating increases from 90 ^oC to 500 ^oC respectively, as in table (2).

The distribution and accumulation of tin dioxide in nanoparticles like to smooth rods (figure 4-c) become large bubbles with an increase in size when annealing at 500 ^oC (figure 4-d). That is mean the product may be converted to tin dioxide nanoparticles during the preparation method (autoclave) and the grain size increases from 48.08 nm to 98.34 nm by increasing temperature as a result of improving the crystalline and the accumulation of the nanoparticles [21], as in table (2).

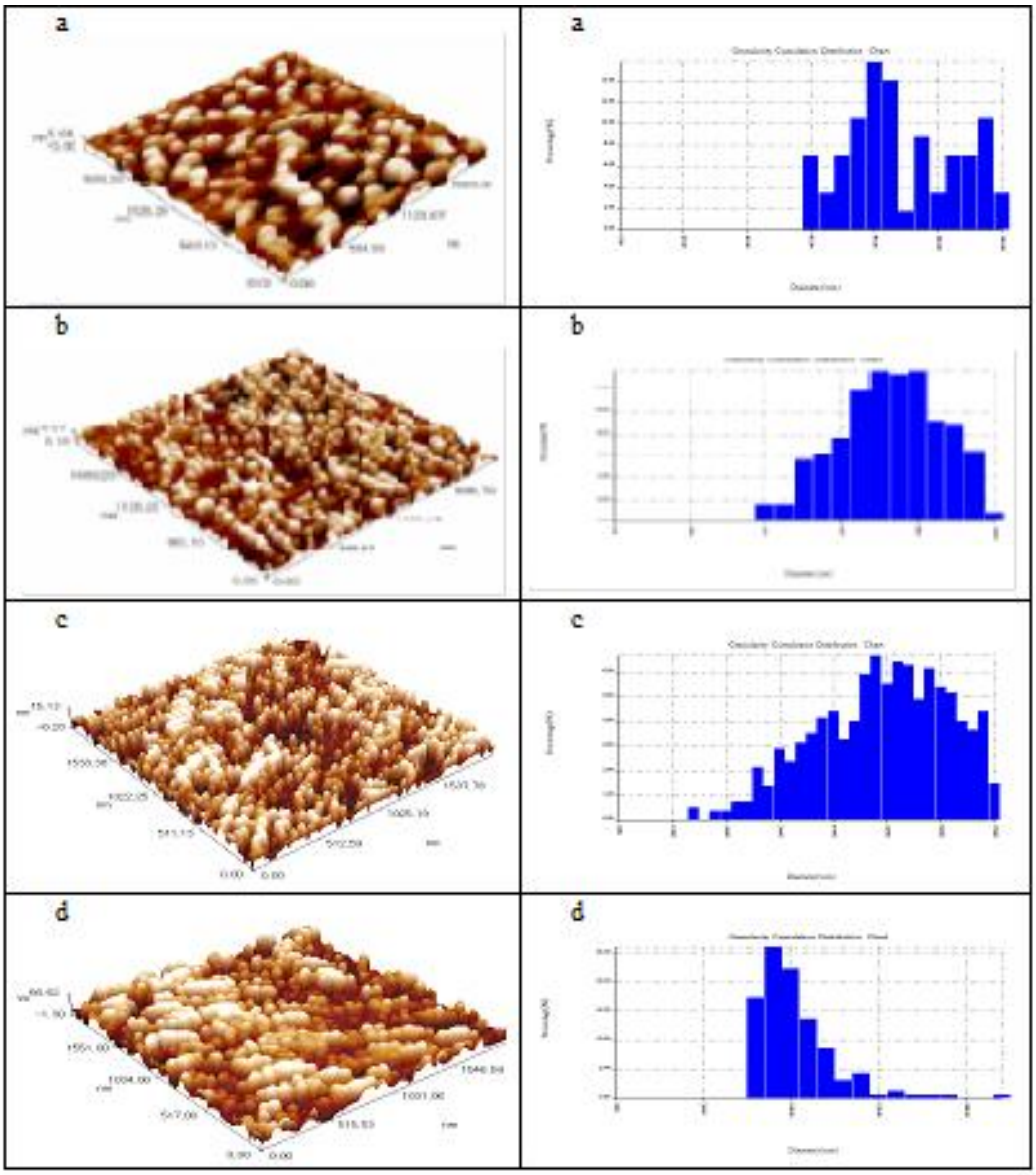

Figure (4): AFM images at 3D of vanadium pentoxide and tin dioxide at different temperatures

Table (2): Average grain size of nanoparticles of V_2O_5 and SnO_2 at (90 °C and 500 °C).

Nanoparticles	Average grain size(d) (nm) heating at	
	90 °C	500°C
Vanadium pentoxide	86.02	70.34
Tin dioxide	48.08	98.34

3.4.2 By Surface scanning Electron Microscopy (SEM)

The surface morphology magnification SEM images of the metal oxides (V_2O_5 and SnO_2) nanoparticles annealing at temperature 500 °C for 120 min, with a magnification of 100 µm, are shown in figures (5). The surface morphology of V_2O_5 (figure 5-a), has a high aggregate consisting of close rough leaves, and that for SnO_2 (figure 5-b) seem to be nanoclusters.

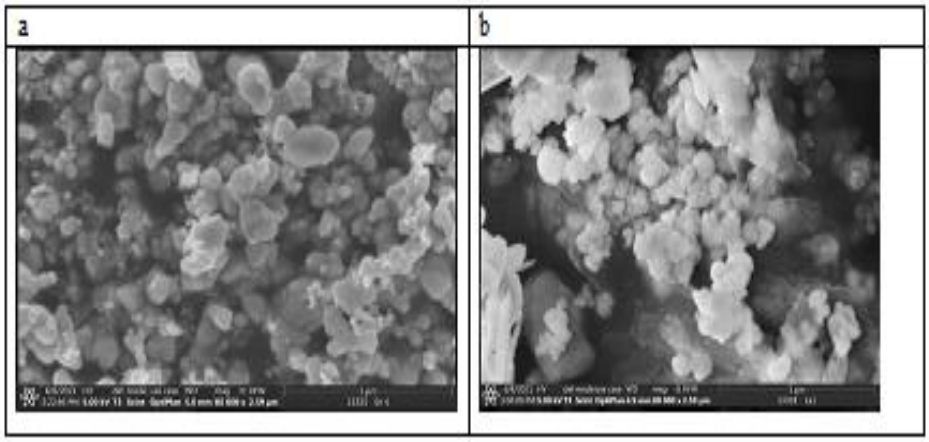

Figure (5): SEM analysis of the surface shape annealing at 500 °C for 120 min: (a) V_2O_5 and (b) SnO_2.

4. Applications

4.1 The adsorptions of methylene blue (MB) dye onto nanoparticles.

Vanadium petoxide ($V_2O_5.nH_2O$) nanoparticles have the highest value of removal percentage (R%) compare with tin dioxide (SnO_2) nanoparticles, as in figure (6). Our results showed that methylene blue dye onto nanoparticles increased sharply during the first 10 min, it may be related to the availability of large bonding sites on the surface area of the nanoparticles. After that, very slow adsorption happens between 10 min to 60 min, this situation continues until the equilibrium happens. While the low increase in adsorption onto nanoparticles takes place (after 10 min), it relates to the aggregation or overlap of the adsorption sites [22]. The annealing at 500 ^oC is similar to the same sequences (to some extent) of the nanoparticles heating at 90 ^oC, except for the result at 50 min (for V_2O_5) which decreases in adsorption compared with the measurements between 10 min to 60 min. This decrease may relate to the dissociation of clusters of dye on the surface of the nanoparticles, as in figure (6). While the removal percentage (R%) for kerosene by V_2O_5 doping onto oxide multiwall carbon nanotube was 80 %. [5].

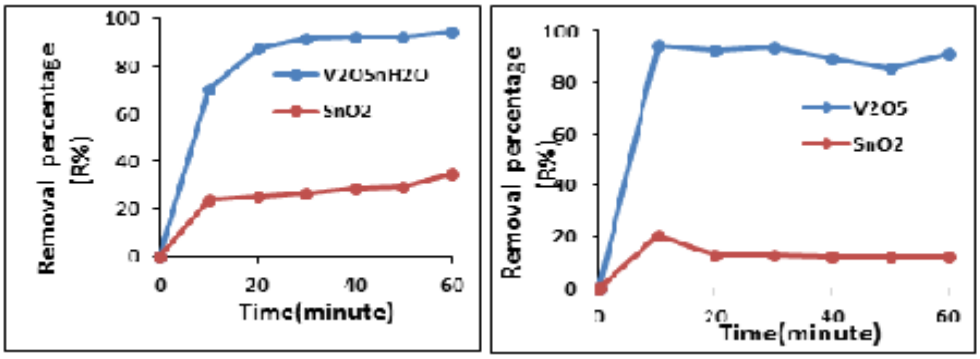

Figure (6): The removal percentage (R%) of MB onto $V_2O_5.nH_2O$ and SnO_2 nanoparticles heating at 90 ˚C and 500 ˚C for 60 min)**.**

When the adsorption capacity (q_t) of MB onto nanoparticles plot against contact time of nanoparticles (heating at 90 ^oC), figure (7), we found the adsorption capacities (q_t) are precisely like the situations that happen in the removal percentage operation (at 90 ^oC), with the identical sequences. As well as the adsorption capacities (q_t) of the samples heated at temperature 500 ^oC, show same the sequences of removal percentage. This similarity is attributed to using of the same volume of dye and the exact weight of nanoparticles in all experiments. Except for the result at 10 min of SnO_2 nanoparticles which gave some increase in removal percentage (q_t) compared with the measurements after that (20 min to 60 min), this increase may relate to providing large surface areas after that dissociation of clusters dyes on the surface of the nanoparticles. As in figure (7). While the adsorption capacity (q_t) for kerosene by V_2O_5 doping onto oxide multiwall carbon nanotube was 10.2 [5].

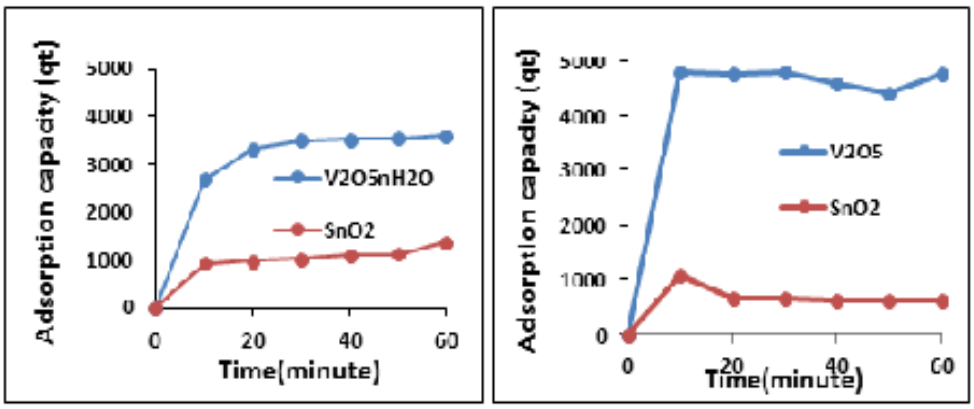

Figure (7): Adsorption capacity (q_t) of MB onto $V_2O_5.nH_2O$ and SnO_2 nanoparticles heating at 90 ˚C and 500 ˚C for 60 min)

4.2 The adsorption of bromothymol blue (BTB) dye onto nanoparticles.

Vanadium petoxide ($V_2O_5.nH_2O$) nanoparticles have the highest value of removal percentage compare with tin dioxide (SnO_2) nanoparticles, as in figure (8). Our results show that the bromothymol blue dye's removal percentage (R%) onto nanoparticles increased sharply during the first 10 min of $V_2O_5.nH_2O$. After that, a prolonged decrease happens between 10 min to 40 min. Then there is a slow increase between 40 min to 60 min. The high increase in adsorption onto nanoparticles in the first 10 min may be related to the availability of large bonding sites on the surface area of the nanoparticles. While the low increase in adsorption onto nanoparticles takes place (between 10 min to 40 min), it may be related to the aggregation or overlap of the adsorption sites, which are the dissociation of clusters of dyes on the surface of the nanoparticles. Then the surface of nanoparticles will get some empty spaces to continue adsorption.

The removal percentage (R%) of the V_2O_5 sample (heating at 500 ^oC) is the highest among other nanoparticles and different that at 90 ^oC. The activity to removal (R%) continues to increase after 10 min and becomes maximum at 40 min. After that, there is a decrease (at 50 min) and a return to increasing (at 60 min), the increase in removal relates to providing large surface areas to bond with dyes molecules. In contrast the decreases in removal relate to the dissociation of clusters of dyes on the surface of the nanoparticles, as in figure (8)

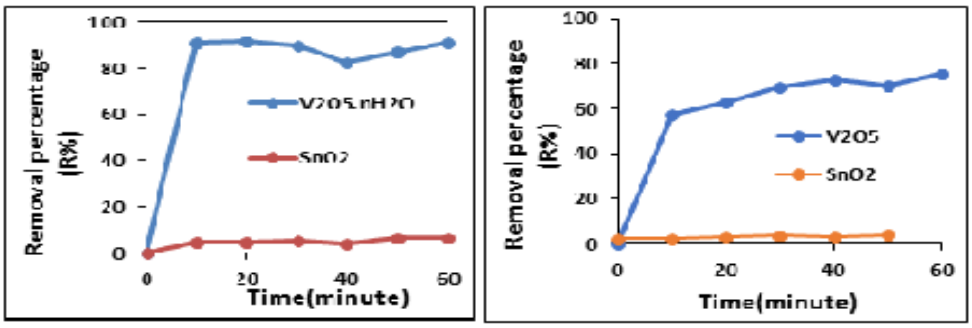

Figure (8): The removal percentage (R%) of BTB onto $V_2O_5.nH_2O$ and SnO_2 nanoparticles heating at 90 ˚C and 500 ˚C for 60 min).

When the adsorption capacity (q_t) of BTB onto nanoparticles plot against contact time of nanoparticles (heating at 90 ^oC), figure (9). The adsorption capacity (q_t) of nanoparticles is a similarity in shape compared to removal percentage (R %) at the same temperature (heating at 90 ^oC). The increase continues (in the V_2O_5 nanoparticles) to get the maximum adsorption capacities (q_t) at 10 min, then began to decrease at 40 min after that the increase continues. The increase in adsorption capacities (q_t), related to nanoparticles' surface will get some empty spaces to bond with dyes molecules. While the decrease relating to the dissociation of clusters dyes on the surface of the nanoparticles.

When the adsorption capacity (q_t) of BTB onto nanoparticles plot against contact time of nanoparticles (heating at 500 ^oC), figure (9), we found the adsorption capacities (q_t) are precisely like the situations that happen in the removal percentage operation (at 500 ^oC), with the identical sequences. This similarity is attributed to the use of the same volume of the dye and the exact weight of nanoparticles in all experiments. The highest adsorption capacities (q_t) where to V_2O_5 nanoparticles. The maximum value of q_t it was at 40 min, may be relate to providing large surface areas after that dissociation of clusters of the dyes on the surface of the nanoparticles.

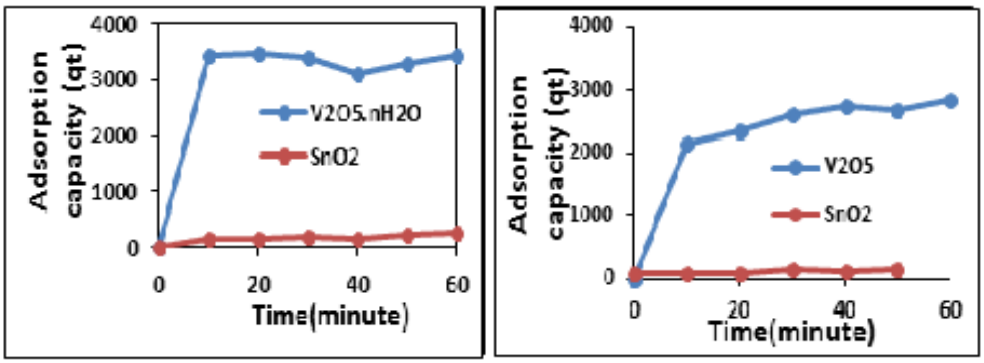

Figure (9): Adsorption capacity (q_t) of BTB onto $V_2O_5.nH_2O$ and SnO_2 nanoparticles heating at 90 ^oC and 500 ^oC for 60 min.

The ability of vanadium pentoxide to adsorb MB or BTB dyes is the largest. This may be related to the ionic potential (charge/radius) of the nanoparticles. The highest ionic potential appears to be vanadium pentoxide (0.073), and the second appears to be tin dioxide (0.048). These results agree with the explanation of removal percentage (R%) sequence and adsorption capacities (q_t) of MB or BTB dyes onto nanoparticles in both situations (90 ^oC and 500 ^oC). Therefore, we can consider that the ionic potential may be the critically affected agent in this operation.

5. Mechanisms to Remove MB and BTB Dyes

5.1 Mechanisms to Remove Methylene blue (MB)

The mechanism to remove Mb from aqueous solution by nanoparticles can be occurredby two methods: first method by the interaction between the positive charge on the sulphur atom of the MB and the partial negative charge on the oxygen atom of the nanoparticle to form an ionic bond. The second method is the interaction between alone pair electrons (as base) on the nitrogen atom of the MB and metal ion (as acid) in the nanoparticles to form a coordination bond [22]. Therefore there is two bonds (ionic and covalent) formation between MB and nanoparticles, as in figure (10) [23].

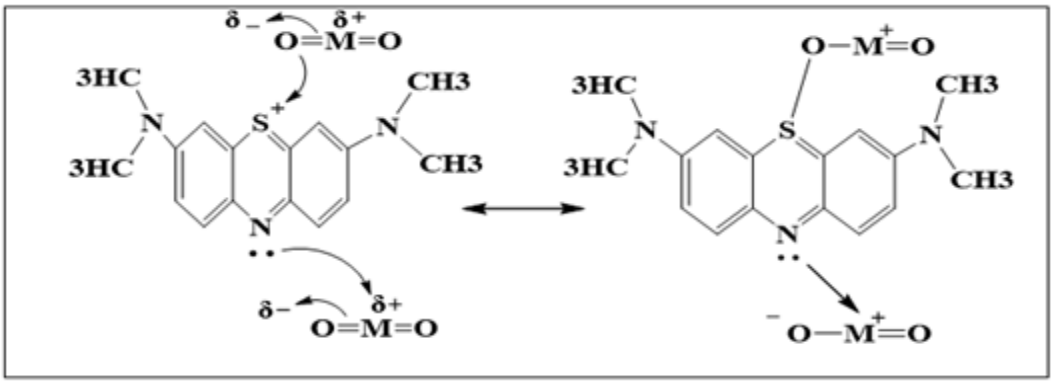

Figure (10): The suggested mechanism to remove methylene blue (MB) by nanoparticles.

5.2 Mechanisms to Remove Bromothymol blue (BTB).

The mechanism to remove BTB from aqueous solution by the nanoparticles can occur through the interaction between the partially positive charges on the metal in the nanoparticle, with a negative charge in the

BTB to form an ionic bond be explained in figure (11).

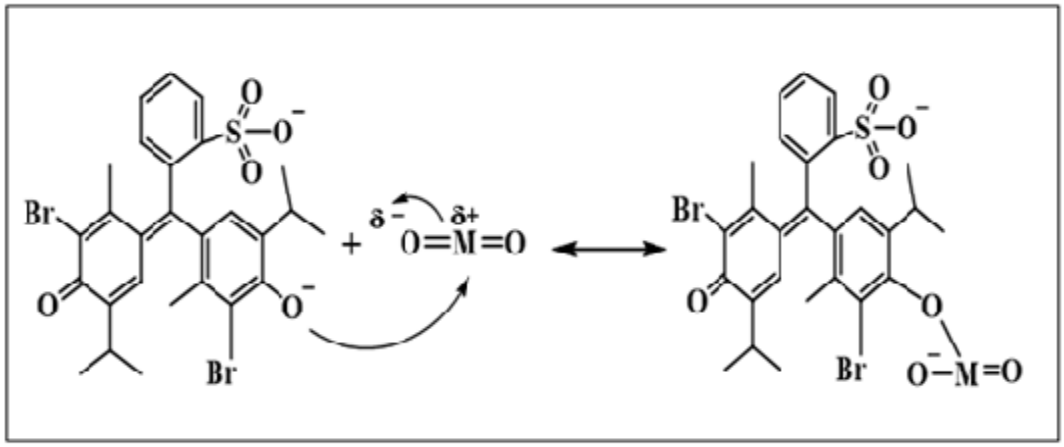

Figure (11): The suggested mechanisms to remove bromothymol blue (BTB) by nanoparticles.

According to these mechanisms, MB can bond with nanoparticles from two sides (sulphur and nitrogen), while BTB can bond with nanoparticles only by one side (phenoxide). Therefore, we can conclude why the removal of nanoparticles by MB is higher than that of BTB.

6. Conclusion

The conclusion can be summarized in the following points:

1. We successfully prepared some nanoparticles ($V_2O_5.nH_2O$ and SnO_2) and their oxides (V_2O_5 and SnO_2) by different methods.
2. After heating temperature at 90 ^oC SnO_2 has the lowest average grain size (48.08) nm.
3. After heating temperature at 500 ^oC, V_2O_5 has the lowest average grain size (70.34) nm,
4. Both $V_2O_5.nH_2O$ and V_2O_5 have the highest removal percentage (R%) and adsorption capacity (q_t) against MB and BTB dyes (as a pollutant), after heating temperatures (90 ^oC and 500 ^oC), and the activity is more when heating at 500 ^oC compared to other nanoparticles.
5. The highest values of R% and q_t for vanadium pentoxide nanoparticles may be relate to the highest ionic potential (0.073). Moreover, we conclude the adsorption may be depend on this factor and do not depend on the average grain size or surface area.

Acknowledgement

We are grateful to Inorganic Lab. Applird Chemistry, App;ied Sciences, University of Technology, for their support of the work.

Conflict of Interest

There is no conflict of interest.

References

[1] X. Qu, , P.J. Alvarez, and Q.J.W.r. Li, "Applications of nanotechnology in water and wastewater treatment", *Water Research*,. vol. 47. p. 3931-3946. 2013.

[2] N. Savage, and M.S.J.J.O.N. Diallo, "Nanomaterials and water purification: opportunities and challenges", *Journal of Nanoparticle Research*, vol. 7. p. 331-342. 2005.

[3] M. Bahrami, and A.J.M.S.i.S.P,Nezamzadeh-Ejhieh, "Effect of the supported ZnO on clinoptilolite nano-particles in the photodecolorization of semi-real sample bromothymol blue aqueous solution", *Materials Science in Semiconductor Processing*. vol. 30. p. 275-284. 2015.

[4] B.K.A. Al–Roos, , S.H. Lubbad, and K.K.J.I.J.o.E.S. Abu–Saqer, "Assessment of thermally treated sphagnum peat moss sorbents for removal of phenol red, bromothymol blue and malachite green from aqueous solutio", *International Journal of Environmental Studies*. vol.76. p. 861-872, 2019.

[5] T. A. Abdullah, Ba-Son Nguyen, T. Juzsakova, R. T. Rasheed, S. Hafad, H. Mansoor, *et al*., "Promotional effect of metal oxides (MxOy = TiO_2, V_2O_5) on multi-walled carbon nanotubes (MWCNTs) for kerosene

removal from contaminated water", *Materials Letters*, 292 (2021).

[6] A.J.I.J.O.E.P. Hasham,. and E. Modelling, "Selected Nanotechnology Applications in Industrial Waste Water Treatme", *Molecules: A Review*, vol. 1. p. 71-76, 2018.

[7] J. Saikia, , A. Gogoi, and S. Baruah, "Nanotechnology for water remediation. Environmental Nanotechnology", *Springer*, vol. 2, p. 195-211, 2019.

[8] D.P. Nair, T Sakthivel, R Nivea, Jeena Susan Eshow, V Gunasekaran., "Effect of surfactants on electrochemical properties of vanadium-pentoxide nanoparticles synthesized via hydrothermal method". *Journal of nanoscience and nanotechnology*. vol. 15. p. 4392-4397, 2015.

[9] R. Rashad Ibraheem, MSc. thesis. "Preparation of V_2O_5 , TiO_2 , CeO_2 nanoparticles and its composites asenzyme mimetics", 2019, University of Technology: IRAQ.

[10] F. Gu, S.F.Wang, M. K. Lu, G. J. Zhou, D. Xu, and D. R.Yuan, "Photoluminescence properties of SnO_2 nanoparticles synthesized by sol− gel method", T*he Journal of Physical Chemistry* B, vol. 108. p. 8119-8123, 2004.

[11] R. T. Rasheed, M. Hadeel S. A, T. Adnan, J. Tatjana, N. Al‐Jammal, A. D.Salman, R. R. Al‐Shaikhly, P. C. Le, E. Domokos, T. A. Abdulla, "Synthesis, characterization of V_2O_5 nanoparticles and determination of catalase mimetic activity by new colorimetric method", *Journal of Thermal Analysis and Calorimetry*. p. 1-11. 2020.

[12] Al-A. Saryia .D., R. Rashed T., and M. Hadeel S., "Preparation, Structural and Optical Properties of SnO_2 Thin Films Prepared by Sol-Gel Method". *Asian Journal of Materials Chemistry*, vol. 2, p. 1-5, 2017.

[13] M. Farahmandjou, and N.J.J.o.N.R. Abaeiyan, "Chemical synthesis of vanadium oxide (V_2O_5) nanoparticles prepared by sodium metavanadate", *Journal of Nanomedicine Research*, vol. 5. p. 00103, 2017.

[14] S. Nalin, B. Selvakumar, and P.J.I.J.E.M.S. Periasamy, *"Simple Synthesis and Characterization of V_2O_5 Nanoparticles by Microwave Assisted Wet Chemical Method* ", I*nternational Journal of Engineering and Manufacturing Science*" vol.2. p. 411-417. 2017.

[15] A. Elci, O. Demirtas, I. M. Ozturk, A. Bek, and E. Nalbant Esenturk, "Synthesis of tin oxide-coated gold nanostars and evaluation of their surface-enhanced Raman scattering activities", *Journal of Materials Science*, vol. 53. p. 16345-16356, 2018.

[16] Hai-Tao Fu, Z. Zhi-Kui, Y. Xiao-Hong, and Xi-Zhong An, "Two-Step Synthesis of V_2O_5 Nanosheets with High Sensing Properties toward Acetone", Advances in Engineering Research, vol. 11, p. 372-379, 2017.

[17] Z. Pengfei, Z. Luzi, An. Qinyou, W., Z. Liang, W. Xiujuan, S. Jinzhi, *et al.*, "A High-Rate V_2O_5 Hollow Microclew Cathode for an All-Vanadium-Based Lithium-Ion" *Full Cell*. Small, vol. 12. p. 1082-1090, 2016.

[18] Li. Zhenyu, Cai Jie, C. Pavel, N. Haitao, Du. Yong and Lin Tong, "A self-supported, flexible, binder-free pseudo-supercapacitor electrode material with high capacitance and cycling stability from hollow, capsular polypyrrole fibers", *Journal of Materials Chemistry ,* vol. 3. p. 16162-16167, 2015.

[19] Y. Veeraswamy, Y. Vijayakumar, and R.R. Reddy, "Growth and Micro Structural Characterization of In_2O_3 Thin Films Prepared by Electron Beam Evaporation Technique", *Journal of Research in Engineering and Technology*. vol. 5. p. 267-272. 2014.

[20] M. Das, and S.J.M.T.P. Roy, "Preparation, Characterization and Properties of Newly Synthesized SnO_2-Polycarbazole Nanocomposite via Room Temperature Solution Phase Synthesis Process", *Materials Today Proceedings*. vol. 18, p. 5438-5446, 2019.

[21] A. B Khatibani,., S. Rozati, and Z.J.A.P.P.A. Bargbidi, "Preparation, Study and Nanoscale Growth of indium oxide thin films". *Acta Physica Polonica A*, vol. 122. p. 220-223, 2012.

[22] C. Karunakaran, , P. Anilkumar, and P.J.C.C.J. Gomathisankar, "Photoproduction of iodine with nanoparticulate semiconductors and insulators", Chemistry Centeral Journal, vol. 5. p. 1-9, 2011. .

[22] T. A. Abdullah, R. T. Rashed, T. Juzsakova, N. Al‐Jammal, M. A. Mallah, L. P. Cuong, *et al*, "Preparation and characterization of MnO_2-based nanoparticles at different annealing temperatures and their application in dye removal from water", International Journal of Environmental Science and Technology, p. 1-14, 2020.

[23] T. A. Abdullah, T. Juzsakova., S. Hafad, R. T. Rasheed, N. Al‐Jammal, M. A. Mallah, A. D. Salman, P. C. Le, E. Domokos, M. Aldulaimi , "Functionalized multi-walled carbon nanotubes for oil spill cleanup from water", *Clean Technologies and Environmental Policy*. 2021.